# Distribution characteristics and clinical significance of infiltrating T cells in the tumor microenvironment of pancreatic cancer

GEN SUN[1*], ZHENGJIANG YANG[2*], KANG FANG[1], YUANPENG XIONG[1], SHUJU TU[1], SIQING YI[1] and WEIDONG XIAO[1]

[1]Department of General Surgery, The First Affiliated Hospital of Nanchang University, Nanchang, Jiangxi 330006; [2]Department of General Surgery, The Affiliated Hospital of Jiujiang College, Jiujiang, Jiangxi 332001, P.R. China

Received July 28, 2022; Accepted March 24, 2023

DOI: 10.3892/ol.2023.13847

**Abstract.** Tumor-infiltrating lymphocytes (TILs) are important components of the tumor microenvironment (TME). However, the distribution characteristics of TILs and their significance in pancreatic cancer (PC) remain largely unexplored. The levels of TILs, including the total number of T cells, cluster of differentiation (CD)4$^+$ T cells, CD8$^+$ cytotoxic T lymphocytes (CTLs), regulatory T-cells (Tregs), programmed cell death protein 1$^+$ T cells and programmed cell death ligand 1 (PD-L1)$^+$ T cells, in the TME of patients with PC were detected using multiple fluorescence immunohistochemistry. The associations between the number of TILs and the clinicopathological characteristics were investigated using $\chi^2$ tests. In addition, Kaplan-Meier survival and Cox regression analyses were used to assess the prognostic value of these TIL types. Compared with paracancerous tissues, in PC tissues, the proportions of total T cells, CD4$^+$ T cells and CD8$^+$ CTLs were markedly decreased, while those of Tregs and PD-L1$^+$ T cells were significantly increased. The levels of CD4$^+$ T cell and CD8$^+$ CTL infiltrates were inversely associated with tumor differentiation. Higher infiltrates of Tregs and PD-L1$^+$ T cells were closely associated with advanced N and TNM stages. It is important to note that the infiltrates of total T cells, CD4$^+$ T cells, Tregs and PD-L1$^+$ T cells in the TME were independent risk factors for the prognosis of PC. PC was characterized by an immunosuppressive TME with a decrease in the number of CD4$^+$ T cells and CD8$^+$ CTLs, and an increase in the number of Tregs and PD-L1$^+$ T cells. Overall, the number of total T cells, CD4$^+$ T cells, Tregs and PD-L1$^+$ T cells in the TME was a potential predictive marker for the prognosis of PC.

*Correspondence to:* Dr Weidong Xiao, Department of General Surgery, The First Affiliated Hospital of Nanchang University, 17 Yongwaizhengjie, Nanchang, Jiangxi 330006, P.R. China
E-mail: frankxwd@126.com

*Contributed equally

*Key words:* pancreatic cancer, tumor immune microenvironment, tumor-infiltrating lymphocytes, programmed cell death protein 1, programmed cell death ligand 1

## Introduction

Pancreatic cancer (PC) is one of the most fatal digestive system malignancies; it exhibits the highest mortality rate and a yearly increase in occurrence throughout the world (1-3). PC has a clinical characteristic of 'three highs and three lows', namely high morbidity, mortality and recurrence rates, and low early diagnosis, resection and 5-year survival rates (2,3). In China, it is estimated that were 134,374 new cases of PC and 131,203 deaths attributed to this disease in 2022 (1). In the United States, the estimated number of new cases and deaths due to PC in 2022 were 62,210 and 48,830, respectively (2). Despite advances in therapeutic strategies, the prognosis of PC remains poor, with an overall 5-year survival rate of 11%, which is the lowest amongst all malignant tumors (2). Diagnosis and treatment of PC remain a challenge; thus, it is of great importance to elucidate the underlying molecular mechanisms of PC development and progression to highlight potential novel targets and treatments.

The tumor microenvironment (TME) is the environment where cancer cells exist and absorb nutrients or interact with other components. The TME encompasses the surrounding immune cells, lymphocytes, bone marrow-derived inflammatory cells, blood vessels, extracellular matrix, fibroblasts and other signaling molecules (4,5). The TME is commonly considered to be a complex ecosystem with immunosuppressive and tumor-promoting functions (4-6). The TME of PC consists of a large number of dense stromal components that can create a favorable microenvironment for PC cell growth and proliferation, including activated pancreatic stellate cells, tumor-associated fibroblasts and other extracellular stroma components (4,6). The presence of multiple types of immune cells in the TME of PC that is both quantitatively and functionally imbalanced is usually characterized by a decrease in the number of cells with antitumor effects and a non-functional or immature phenotype and state, such as cluster of differentiation (CD)4$^+$ T cells, CD8$^+$ T cells and natural killer (NK) cells, while cells with immunosuppressive effects are functionally active and present in large numbers, such as regulatory T cells (Tregs), myeloid-derived

suppressor cells (MDSCs) and tumor-associated macrophages (TAMs) (4,6). For example, hsa_circ_0046523 can decrease the ratio of $CD4^+$ and $CD8^+$ T cells, and increase the ratio of Tregs by sponging the miR-148a-3p/PD-L1 axis, while accelerating the apoptosis and failure of $CD8^+$ T cells (7). Kaneda *et al* (8) demonstrated that activation of PI3Kγ signaling promotes immunosuppression and tumor growth, while inactivation restores $CD8^+$ T cell activation and cytotoxicity. The research from Kabashima *et al* (9) concluded that patients with PC co-expressing cGAS and STING showed favorable survival outcomes, with several cytotoxic $CD8^+$ T cell infiltrates around the cancer cells, but not in patients with defective cGAS-STING signaling. Lefler *et al* (10) found that the STAT3 signaling axis was disrupted via genetic ablation of STAT3, resulting in a decreased number of M2 macrophages and an increased number of $CD8^+$ T cells, as well as a slowing tumor progression. The PC cells themselves can also promote the activation of surrounding stromal cells and the accumulation of immunosuppressive cells at the tumor site by secreting various cytokines, such as IL-10, TGF-β, chemokines, CXCLl-3 and CXCL5 (5). These multiple factors lead to an imbalance in the number and function of immune effector cells together, forming a unique immunosuppressive microenvironment in PC. A number of emerging studies have revealed that the heterogeneity and complexity of the TME are responsible not only for the growth, invasion and metastasis of PC, but also for its recurrence and resistance to chemotherapy and immunotherapy.

Tumor-infiltrating lymphocytes (TILs) are considered to be one of the major components present in the TME, which primarily includes immune cells, such as T lymphocytes, B lymphocytes and NK cells. As these TILs with different phenotypes exhibit an imbalance in their quantity and function, the interaction of cancer cells, immune cells and cytokines results in a TME that is conducive to tumor cell proliferation, migration and evasion of immune surveillance, which leads to enhanced proliferation and metastasis of PC cells, and increased differentiation and malignancy (5,6). Moreover, TILs can also be used to predict the prognosis and response to immunotherapy in patients with PC (11). Cluster of differentiation (CD)$8^+$ cytotoxic T lymphocytes (CTLs) are considered to be a common type of T lymphocytes present in the TME, which contribute to an excellent cancer prognosis by killing tumor cells (12). $CD8^+$ CTLs cells in the TME are usually supported by $CD4^+$ T helper 1 cells ($CD4^+$ Th1) that release IFN-γ and IL-2 (13). Recently, a systematic review and meta-analysis demonstrated that a high infiltration of $CD8^+$ lymphocytes, $CD3^+$ T cells and $CD4^+$ lymphocytes indicated improved overall survival (OS) rate and disease-free survival (DFS) rate of patients with pancreatic ductal adenocarcinoma (14). Tregs are a specific class of $CD4^+$ T cells that are considered to promote tumor growth and invasion by inhibiting the host's immune response (15). Forkhead box P3 (FOXP3) is one of the most specific markers of Tregs; its elevated expression in Tregs is associated with poor OS and recurrence rates in patients with PC (14,16). By contrast, as a co-stimulatory signaling pathway of the T-cell immune response, the programmed cell death protein 1/programmed cell death ligand 1 (PD-1/PD-L1) pathway plays a crucial role in the immune escape of tumor cells. Previous studies have shown that PD-1 expression is upregulated in tumor-infiltrating $CD8^+$ T cells in several types of solid tumors, and $PD\text{-}1^+$ $CD8^+$ T cells contribute to impaired antitumor immune responses and poor survival outcomes (17,18). Nomi *et al* (19) reported that the positive rate of PD-L1 protein expression was 39.2% in PC tissues and that the expression levels of PD-L1 were inversely correlated with the number of TILs, notably with regard to $CD8^+$ T cells. More importantly, the OS rate of PD-L1-positive patients was significantly lower than that of PD-L1-negative patients. Apparently, the different phenotypes and locations of TILs indicate different survival outcomes. However, the distribution characteristics and the significance of TILs in PC remain largely unexplored.

In the current study, the levels of TILs, including the total number of T cells, $CD4^+$ T cells, $CD8^+$ CTL, Tregs, $PD\text{-}1^+$ T cells and $PD\text{-}L1^+$ T cells, were detected in the TME of patients with PC using multiple fluorescence immunohistochemistry (mFIHC). Furthermore, the relationships between TILs and the clinicopathological features were investigated. Finally, the prognostic value of these TILs was assessed in patients with PC. These findings may provide novel insights into the prognostic evaluation and therapy of PC.

## Materials and methods

*PC tissue microarrays (TMAs).* A commercially available PC TMA was obtained from Shanghai Outdo Biotech Co., Ltd., (https://www.superchip.com.cn/biology/tissue.html; cat no. HPanA150Su01), which contained tumor tissues from 90 patients with PC. This TMA had a total number of 150 points, including 60 pairs of PC tissues and matched paracancerous tissues, and 30 solitary PC tissues. All patients underwent radical resection between September 2004 and December 2008, and were followed up until December 2011.

*mFIHC.* The Opal 7-Color Manual IHC Kit (PerkinElmer, Inc.) was used for mFIHC staining, which enables the simultaneous visualization of six markers and a nuclear counterstain in the same section. The detection panel included CD3, CD4, CD8, FOXP3, PD-1 and PD-L1. Briefly, the TMA was deparaffinized and rehydrated with serial dilution solutions following washing in xylene and graded ethanol. Antigen retrieval was performed by boiling in the antigen retrieval solution (Tris-EDTA Buffer, pH 9.0). Subsequently, the TMA was incubated in 3% hydrogen peroxide solution for 15 min at room temperature to block endogenous peroxidase activity, followed by washing in PBS and incubation with 10% goat serum for 30 min at room temperature. Subsequently, the TMA was incubated with primary antibody (Table I) at 4˚C for 15 h, followed by the addition of horseradish peroxidase (HRP)-conjugated secondary antibodies (Table I) for 30 min at 37˚C. Subsequently, the TMA was incubated with Tyramide signal amplification (TSA)-Opal fluorophores for 10 min at 37˚C and prepared for the next round of staining (the fluorescent markers and corresponding colors are shown in Table I). Between each round of staining, the antibody-TSA complex was removed from the antigen retrieval buffer solution (pH 9) and boiled. Following the last round of antibody staining, the TMA was counterstained with 4',6-diamidino-2-phenylindole (DAPI) for 5 min at room temperature and incubated with

Table I. Primary and secondary antibodies, and fluorescent dyes used in the present study.

A, Primary antibodies

| Antibodies | Dilution | Fluorescent dye | Deposition color | Species | Supplier | Cat. no. |
|---|---|---|---|---|---|---|
| CD3 | 1:500 | Opal 520 | Green | Mouse | Abcam | Ab135372 |
| CD4 | 1:5 (ready to use) | Opal 570 | Cyan | Mouse | Abcam | Ab183685 |
| CD8 | 1:300 | Opal 650 | Red | Mouse | Abcam | Ab217344 |
| FOXP3 | 1:500 | Opal 690 | Pink | Rabbit | Cell Signaling Technology, Inc. | 98377s |
| PD-1 | 1:500 | Opal 540 | Yellow | Mouse | Cell Signaling Technology, Inc. | 86163T |
| PD-L1 | 1:300 | Opal 620 | Magenta | Mouse | Cell Signaling Technology, Inc. | 13684T |

B, Secondary antibodies

| Antibodies | Dilution | Fluorescent dye | Deposition color | Species | Supplier | Cat. no. |
|---|---|---|---|---|---|---|
| HRP-Conjugated AffiniPure Goat IgG Anti-rabbit (H+L) | 1:10,000 | | | | Wuhan Bode Bioengineering Co., Ltd. | BA1051 |
| HRP-Conjugated AffiniPure Goat Anti-mouse IgG (H+L) | 1:10,000 | | | | Wuhan Bode Bioengineering Co., Ltd. | BA1056 |

CD, cluster of differentiation; PD-1, programmed cell death protein 1; PD-L1, programmed cell death ligand 1; FOXP3, forkhead box P3.

ProLong Gold Antifade Reagent (Thermo Fisher Scientific, Inc.). TSA technology was applied to mFIHC in this process, in which the HRP conjugated to the secondary antibody catalyzes the addition of fluorescein substrate to the system, and the production of activated fluorescent substrate that can covalently bind to tyrosine in the vicinity of the antigen, generating a large number of stable fluorescent compounds for signal amplification. Finally, the stained TMA was scanned using the PerkinElmer Vectra (PerkinElmer, Inc.) multispectral imaging platform.

*TIL markers and mFIHC analysis*. The phenotype markers used for targeting TILs were as follows: Total T cells, $CD3^+$; $CD4^+$ T cells, $CD3^+CD4^+$; $CD8^+$ CTLs, $CD3^+CD8^+$; Tregs, $CD3^+CD4^+FOXP3^+$; PD-$1^+$ T cells, $CD3^+$PD-$1^+$; and PD-$L1^+$ T cells, $CD3^+$PD-$L1^+$. At a magnification of x200, one image was captured for each core. The collected original mFIHC images were imported into the inForm image analysis software (version 2.1; PerkinElmer, Inc.), and the colors of the corresponding antibody marker were added; all photos were segmented and the resulting fluorescent images were exported. Subsequently, different antibody markers were labeled, the software automatically identified tissue areas on the image as well as fluorescence, while adjusting the threshold to the optimal value. The corresponding T cell number was then obtained by counting the double or triple-stained cells and the total number of DAPI-labeled nuclei for the total number of cells. Based on the results of the image analysis, the percentage of total T cells, $CD4^+$ T cells, $CD8^+$ CTL, Tregs, PD-$1^+$ T cells and PD-$L1^+$ T cells in the PC tissues and paracancerous tissues was calculated, as well as the percentage of $CD4^+$ T cells, $CD8^+$ CTL, Tregs, PD-$1^+$ T cells and PD-$L1^+$ T cells over the total percentage of T cells.

*Statistical analysis*. SPSS version 24.0 (IBM Corp.) and GraphPad Prism version 8.0 (GraphPad Software; Dotmatics) software were used for statistical analysis. The data are presented as the mean ± standard deviation and compared using an unpaired Student's t-test. The association between the number of TILs and the clinicopathological characteristics was analyzed using a $\chi^2$ test. A Kaplan-Meier survival curve was used to evaluate the relationship between the expression levels of TIL-specific markers and the OS rate, followed by the log-rank test. The forward stepwise Cox regression model was used to perform univariate and multivariate analyses for the assessment of disease prognosis. $P<0.05$ was considered to indicate a statistically significant difference.

## Results

*Patient characteristics*. The results of mFIHC indicated that 57 pairs of PC and matched paracancerous tissues and 25 cases

Table II. Information on 82 cases of patients with pancreatic cancer.

| Variables | Value |
|---|---|
| Median age (range), years | 62 (34-83) |
| Sex, n | |
| Male | 53 |
| Female | 29 |
| Surgical method, n | |
| Pancreatoduodenectomy | 47 |
| Distal pancreatectomy | 30 |
| Tumor enucleation | 5 |
| Tumor location[a], n | |
| Head | 46 |
| Body or tail | 31 |
| Mean tumor size ± SD, cm | 4.7±2.1 |
| T stage[b], n | |
| T1/T2 | 65 |
| T3 | 16 |
| N stage[a], n | |
| N0 | 45 |
| N1 | 32 |
| TNM stage[a], n | |
| I | 36 |
| II | 40 |
| III | 0 |
| IV | 1 |
| Survival, average (range), months | 20.9 (0.6-81) |

A total of 82 pancreatic cancer patients whose tissues were successfully stained using multiplex fluorescence immunohistochemistry were included in this study. [a]5 cases lacked information; [b]1 case lacked information.

of solitary PC tissues with complete tissue structure and no loss in the TMA were successfully stained. The dots circled highlighted in red in Fig. S1 were unsuccessfully stained due to incomplete tissue structure or severe loss. A total of 82 patients with PC were therefore included in the present study, consisting of 53 males and 29 females with a median age of 62 years (34-83 years). Among these cases, 46 of the tumors were located in the head, 31 in the body or tail, and 5 were of unknown location due to a lack of information. The average maximum diameter of the tumors was 4.7±2.1 cm. According to TNM stage classification for PC (eighth edition) (20), 36 tumors were categorized as stage I, 40 as stage II, 1 as stage IV and 5 as unknown due to a lack of information. The patients were followed up for 0.6-87 months until December 2011. At the end of the follow-up, 61 patients succumbed to the disease and 21 patients survived. The average survival time was 21.4±22.7 months (Table II).

*Distribution characteristics of TILs in the TME of PC*. Fig. 1 represents the mFIHC staining pattern of CD3, CD4, CD8, PD-1, PD-L1 and FOXP3 in PC and matched paracancerous

Table III. Percentage of tumor-infiltrating lymphocytes in 57 pairs of PC and matched paracancerous tissues[a].

| Variable | Mean | SD | P-value |
|---|---|---|---|
| Total T cells | | | 0.008[b] |
| Tumor tissues | 5.27 | 4.0 | |
| Paracancerous tissues | 7.69 | 5.4 | |
| $CD4^+$ T cells | | | 0.005[b] |
| Tumor tissues | 0.67 | 0.7 | |
| Paracancerous tissues | 1.14 | 1.0 | |
| $CD8^+$ CTLs | | | <0.001[c] |
| Tumor tissues | 0.21 | 0.4 | |
| Paracancerous tissues | 1.93 | 3.4 | |
| Tregs | | | 0.001[c] |
| Tumor tissues | 0.27 | 0.5 | |
| Paracancerous tissues | 0.04 | 0.1 | |
| PD-$1^+$ T cells | | | 0.712 |
| Tumor tissues | 1.43 | 1.4 | |
| Paracancerous tissues | 1.52 | 1.3 | |
| PD-$L1^+$ T cells | | | 0.032[d] |
| Tumor tissues | 2.38 | 1.6 | |
| Paracancerous tissues | 1.76 | 1.4 | |

[a]In 57 of 60 pairs, staining of PC and matched paracancerous tissues was successful. [b]P≤0.01, [c]P≤0.001, [d]P≤0.05. PC, pancreatic cancer; CD, cluster of differentiation; PD-1, programmed cell death protein 1; PD-L1, programmed cell death ligand 1; Treg, regulatory T cell.

Table IV. Percentage of different tumor-infiltrating lymphocytes over the number of total T cells in 57 pairs of pancreatic cancer and matched paracancerous tissues[a].

| Variables | Mean | SD | P-value |
|---|---|---|---|
| $CD4^+$ T cells | | | 0.104 |
| Tumor tissues | 14.7 | 10.5 | |
| Paracancerous tissues | 18.8 | 16.0 | |
| $CD8^+$ CTLs | | | <0.001[b] |
| Tumor tissues | 3.5 | 5.4 | |
| Paracancerous tissues | 22.2 | 21.5 | |
| Tregs | | | <0.001[b] |
| Tumor tissues | 5.2 | 4.0 | |
| Paracancerous tissues | 0.6 | 1.1 | |
| PD-$1^+$ T cells | | | 0.110 |
| Tumor tissues | 25.6 | 10.0 | |
| Paracancerous tissues | 22.0 | 14.2 | |
| PD-$L1^+$ T cells | | | <0.001[b] |
| Tumor tissues | 48.2 | 16.8 | |
| Paracancerous tissues | 25.2 | 15.3 | |

[a]In 57 of 60 pairs, staining of pancreatic cancer and matched paracancerous tissues was successful. [b]P<0.001. CD, cluster of differentiation; PD-1, programmed cell death protein 1; PD-L1, programmed cell death ligand 1; Treg, regulatory T cell.

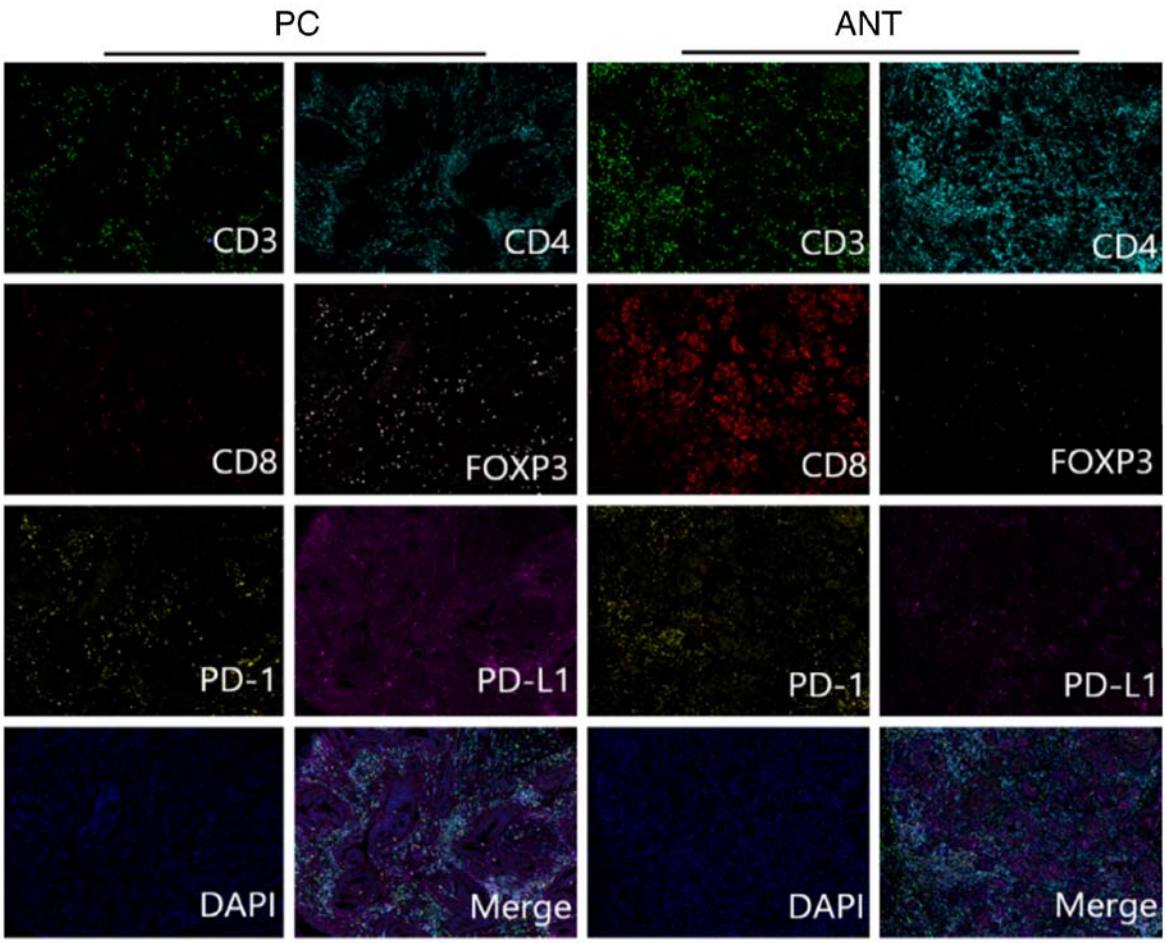


Figure 1. Multiplex fluorescence immunohistochemistry staining of CD3 (green), CD4 (cyan), CD8 (red), PD-1 (yellow), PD-L1 (magenta), FOXP3 (pink) and DAPI (blue) in PC tissues and ANT. Representative merged images of the PC tissues and ANT, respectively, are shown from 1 patient following multispectral merging. Scale bar, 200 $\mu$m. CD, cluster of differentiation; PD-1, programmed cell death protein 1; PD-L1, programmed cell death ligand 1; FOXP3, forkhead box P3; DAPI, 4',6-diamidino-2-phenylindole; PC, pancreatic cancer; ANT, adjacent normal tissues.

tissues. As shown in Table III, the percentage of total T cells (Fig. 2A), $CD4^+$ T cells (Fig. 2B) and $CD8^+$ CTLs (Fig. 2C) in the PC tissues was significantly lower compared with that noted in the paracancerous tissues, while the percentage of Tregs (Fig. 2D) and PD-$L1^+$ T (Fig. 2F) cells in PC tissues was significantly increased. However, the percentage of PD-$1^+$ T cells demonstrated no significant difference between PC and paracancerous tissues (Fig. 2E). Moreover, the proportion of $CD8^+$ CTLs in the total number of T cells was significantly reduced (Fig. 2H), while the proportion of Tregs (Fig. 2I) and PD-$L1^+$ T (Fig. 2K) cells in the total number of T cells was significantly increased in PC tissues. Finally, the proportion of $CD4^+$ T (Fig. 2G) cells and PD-$1^+$ T (Fig. 2J) cells in the total number of T cells was comparable between PC and paracancerous tissues (Table IV).

*Association of TILs with clinicopathological characteristics.* The median number of each TIL type was used as a cut-off point to classify the patients included in the study into low- and high-infiltration groups. The associations of TILs with clinicopathological characteristics were analyzed. As shown in Tables V-VII, the extent of infiltration of the total number of T cells was closely associated with the tumor differentiation and T stage, but not with sex, age, tumor diameter, N stage and TNM stage. The infiltrates of $CD4^+$ T cells and $CD8^+$ CTLs were inversely associated with tumor differentiation. Higher infiltrates of Tregs and PD-$L1^+$ T cells were closely associated with advanced N and TNM stages. The levels of PD-$1^+$ T cell infiltration were closely associated with tumor differentiation and T stage, and were not associated with sex, age, tumor diameter, N stage and TNM stage.

*Association of TILs with prognosis.* Kaplan-Meier analysis indicated that patients with high levels of total T cell (Fig. 3A, P=0.010), $CD4^+$ T cell (Fig. 3B, P=0.021), and $CD8^+$ CTL (Fig. 3C, P=0.015) infiltrates exhibited a significantly higher OS rate than those with low levels of infiltrates. However, the OS rate of patients with high levels of Treg (Fig. 3D, P=0.036) and PD-$L1^+$ T cell (Fig. 3F, P=0.005) infiltrates was significantly lower than that of patients with low levels of Treg and PD-$L1^+$ T cell infiltrates. In addition, the infiltrate levels of PD-$1^+$ T cells exhibited no significant effect on the OS rate (Fig. 3E, P=0.677).

*Multivariate analysis of prognosis in patients with PC.* Univariate analysis indicated that tumor differentiation (P=0.010), N stage (P=0.007), TNM stage (P=0.004), total number of T cells (P=0.010), $CD4^+$ T cells (P=0.021), $CD8^+$

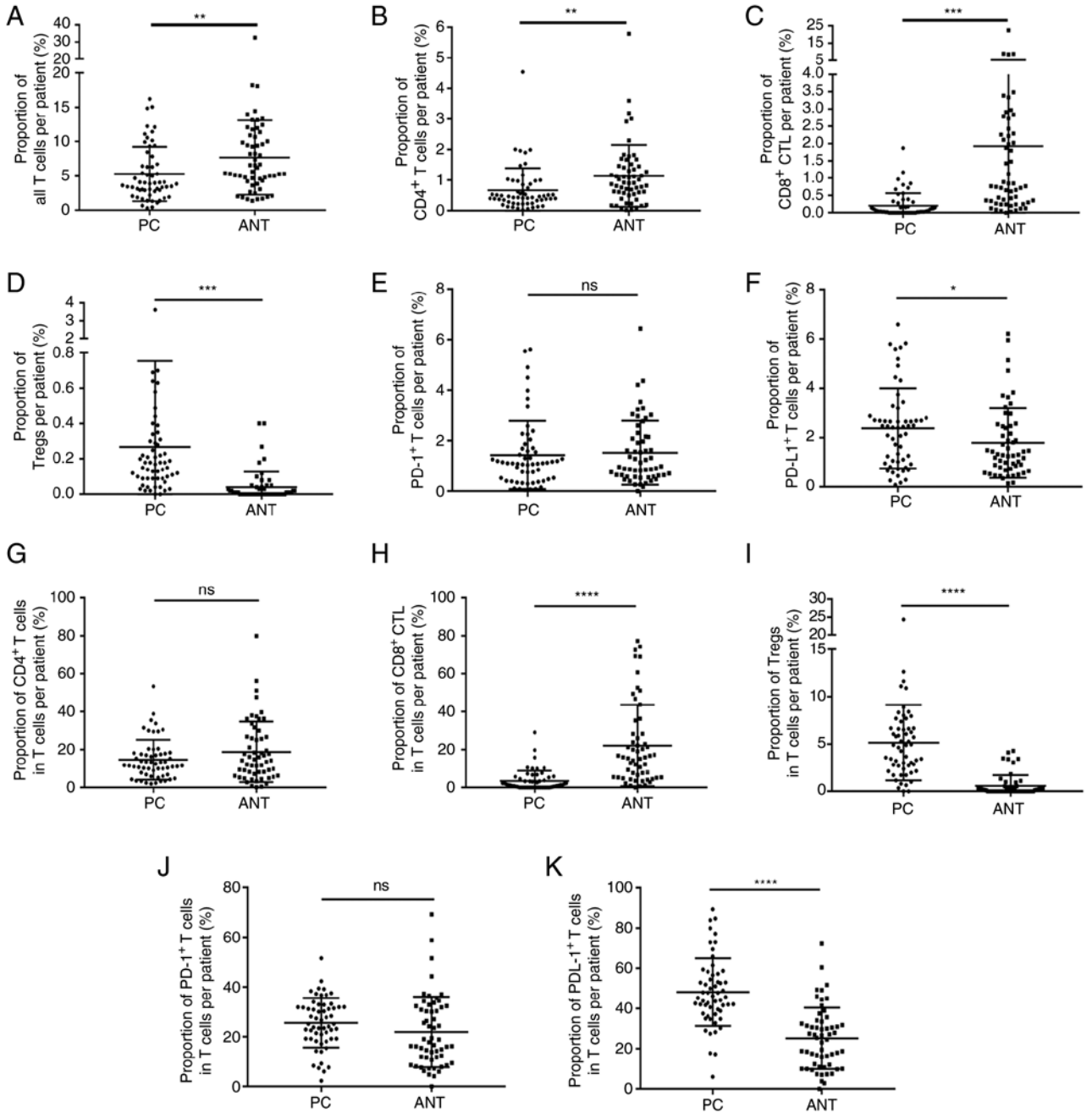


Figure 2. Percentage of TILs and the percentage of TILs over the total percentage of T cells in the PC tissues and ANT. (A-F) The percentage of (A) total T cells, (B) $CD4^+$ T cells and (C) $CD8^+$ CTLs in PC tissues were significantly reduced compared with those in ANTs, while those of (D) Tregs and (F) $PD\text{-}L1^+$ T cells in the PC tissues were significantly increased; in (E) $PD\text{-}1^+$ T cells no significant difference was noted. (G-K) The percentage of (H) $CD8^+$ CTLs as a percentage of total T cells was significantly reduced, while the percentage of (I) Tregs and (K) $PD\text{-}L1^+$ T cells was markedly increased in PC tissues; the proportion of (G) $CD4^+$ T cells and (J) $PD\text{-}1^+$ T cells did not differ significantly. $^*P<0.05$, $^{**}P<0.01$, $^{***}P<0.001$, $^{****}P<0.0001$. ns, not significant; TILs, tumor-infiltrating lymphocytes; PC, pancreatic cancer; ANTs, adjacent normal tissues; CD, cluster of differentiation; CTLs, cytotoxic T lymphocytes; Tregs, T regulatory cells; PD-L1, programmed cell death ligand 1; PD-1, programmed cell death protein 1.

CTLs (P=0.015), Tregs (P=0.036) and $PD\text{-}L1^+$ T cells (P=0.005) were associated with the OS rate of patients with PC (Table VIII). Subsequently, these variables were included in a multivariate Cox regression model. Multivariate analysis revealed that tumor differentiation [hazard ratio (HR), 2.733; P=0.001], TNM stage (HR, 2.364; P=0.005), total number of T cells (HR, 0.323; P=0.001), $CD4^+$ T cells (HR, 0.393; P=0.003), $PD\text{-}L1^+$ T cells (HR, 2.305; P=0.012) and Tregs (HR, 2.786; P=0.003) were independent risk factors of OS rate in patients with PC (Table IX).

## Discussion

Despite the improvements in the survival times of patients with PC due to radical resection combined with adjuvant chemotherapy, the prognosis of patients with PC remains extremely poor, as ~50% of patients are diagnosed in the first instance with advanced-stage disease. In recent years, immunotherapy consisting of PD-1 and PD-L1 inhibitors has been shown to be highly effective in the treatment of melanoma, non-small cell lung cancer and hepatocellular carcinoma (21,22).

Table V. Associations of total number of T cells and CD4+ T cells with clinicopathological characteristics in 82 cases of pancreatic cancer.

| | Total T cells, n (%) | | | CD4+ T cells, n (%) | | |
|---|---|---|---|---|---|---|
| Variables | Low (n=41) | High (n=41) | P-value | Low (n=41) | High (n=41) | P-value |
| Sex | | | 0.106 | | | 0.817 |
| Male | 30 (56.60) | 23 (43.40) | | 27 (50.94) | 26 (49.06) | |
| Female | 11 (37.93) | 18 (62.07) | | 14 (48.28) | 15 (51.72) | |
| Age, years | | | 0.267 | | | 0.506 |
| ≤60 | 16 (43.24) | 21 (56.76) | | 17 (45.95) | 20 (54.05) | |
| >60 | 25 (55.56) | 20 (44.44) | | 24 (53.33) | 21 (46.67) | |
| Diameter, cm[a] | | | 0.860 | | | 0.503 |
| ≤3 | 12 (52.17) | 11 (47.83) | | 13 (56.52) | 10 (43.48) | |
| >3 | 29 (50.00) | 29 (50.00) | | 28 (48.28) | 30 (51.72) | |
| Differentiation | | | 0.040[b] | | | 0.012[b] |
| Well/moderately differentiated | 21 (41.18) | 30 (58.82) | | 20 (39.22) | 31 (60.78) | |
| Poor | 20 (64.52) | 11 (35.48) | | 21 (67.74) | 10 (32.26) | |
| T stage[a] | | | 0.049[b] | | | 0.615 |
| T1/T2 | 29 (44.62) | 36 (55.38) | | 32 (49.23) | 33 (50.77) | |
| T3 | 12 (75.00) | 4 (25.00) | | 9 (56.25) | 7 (43.75) | |
| N stage[c] | | | 0.271 | | | 0.271 |
| N0 | 24 (53.33) | 21 (46.67) | | 24 (53.33) | 21 (46.67) | |
| N1 | 13 (40.63) | 19 (59.37) | | 13 (40.63) | 19 (59.37) | |
| TNM stage[c] | | | 0.891 | | | 0.749 |
| I | 17 (47.22) | 19 (52.78) | | 18 (50.00) | 18 (50.00) | |
| II-IV | 20 (48.78) | 21 (51.22) | | 19 (46.34) | 22 (53.66) | |

[a]1 case lacked information; [b]P<0.05; [c]5 cases lacked information. CD, cluster of differentiation.

However, the treatment of PC remains a challenge due to the disappointing results derived from immunotherapy (5). This failure is likely due to a highly immunosuppressive TME state present in PC. TILs are important components of the TME and their composition reflects the confrontation between the host immune system and the tumor cells (23). Among these TILs, CD4+ T cells and CD8+ CTLs are the primary antitumor effector T cells, and they can inhibit the occurrence and progression of cancer through various mechanisms. Upon activation, CD4+ T cells can differentiate into CD4+ Th1 cells and secrete IL-2 to activate CD8+ CTLs. Subsequently, cytokines, such as IFN-γ, TNF-β, IL-4, IL-5 and IL-10 are secreted by CD8+ CTLs, and regulate cellular and humoral immunity for killing or inhibiting the progression of PC tumor cells (24,25). Previous studies have shown that patients with PC and high levels of infiltrating CD4+ T cells and CD8+ CTLs in tumor tissues present with an improved prognosis (23,26). Recently, spatial computational analysis revealed that the density of CD8+ cells throughout the tumor and tumor center was associated with higher survival rates in patients with PC (27). Moreover, evidence has also indicated that patients with PC with a substantial level of CD8+ CTL infiltrate exhibit an improved response to chemotherapy (28). Similarly, TILs are present in the TME of other malignancies. For example, higher levels of CD8+ CTLs were observed in the tumor tissues of patients with cervical and ovarian cancer, and were associated with improved patient prognosis (29,30). The increase in the Treg count was associated with colorectal cancer tumor progression, immunotherapy failure and a poorer prognosis (31,32). In the present study, the distribution characteristics of six types of TILs were investigated in PC tissues using mFIHC. The results demonstrated that the infiltrate levels of the total number of T cells, CD4+ T cells and CD8+ CTLs were significantly reduced, while the number of Tregs and PD-L1+ T cells was significantly increased in PC tissues. Moreover, higher levels of total T cells, and CD4+ T cell and CD8+ CTL infiltrates were associated with an improved prognosis, whereas higher levels of Treg and PD-L1+ T cell infiltrates in the tumor tissues were indicative of a poorer prognosis in the patients with PC. The Cox regression model with multivariate analysis indicated that the levels of total T cells, and CD4+ T cell, Treg and PD-L1+ T cell infiltrates, as well as the tumor differentiation and TNM stage, were independent risk factors for the OS rate of patients with PC. These results suggested that the decreased number of CD4+ T cells and CD8+ CTLs, as well as the increased number of Tregs and PD-L1+ T cells in the tumor tissues, contributed to the formation of an immunosuppressive TME state in patients with PC.

Tregs are a subgroup of CD4+ T cells, which are one of the most important immunosuppressive cells present in the

Table VI. Association between the percentage of $CD8^+$ CTLs and Tregs with the clinicopathological characteristics in the 82 cases of pancreatic cancer.

| | $CD8^+$ CTLs, n (%) | | | Tregs, n (%) | | |
|---|---|---|---|---|---|---|
| Variables | Low (n=41) | High (n=41) | P-value | Low (n=41) | High (n=41) | P-value |
| Sex | | | 0.817 | | | 0.488 |
| Male | 26 (49.06) | 27 (50.94) | | 28 (52.83) | 25 (47.17) | |
| Female | 15 (51.72) | 14 (48.28) | | 13 (44.83) | 16 (55.17) | |
| Age, years | | | 0.824 | | | 0.824 |
| ≤60 | 19 (51.35) | 18 (48.65) | | 19 (51.35) | 18 (48.65) | |
| >60 | 22 (48.89) | 23 (51.11) | | 22 (48.89) | 23 (51.11) | |
| Diameter, cm[a] | | | 0.245 | | | 0.418 |
| ≤3 | 14 (60.87) | 9 (39.13) | | 10 (43.48) | 13 (56.52) | |
| >3 | 27 (46.55) | 31 (53.45) | | 31 (53.45) | 27 (46.55) | |
| Differentiation | | | 0.012[b] | | | 0.111 |
| Well, moderately, and highly differentiated | 20 (39.22) | 31 (60.78) | | 22 (43.14) | 29 (56.86) | |
| Poorly differentiated | 21 (67.74) | 10 (32.26) | | 19 (61.29) | 12 (38.71) | |
| T stage[a] | | | 0.162 | | | 0.615 |
| T1/T2 | 30 (46.15) | 35 (53.85) | | 32 (49.23) | 33 (50.77) | |
| T3 | 11 (68.75) | 5 (31.25) | | 9 (56.25) | 7 (43.75) | |
| N stage[c] | | | 0.307 | | | 0.004[d] |
| N0 | 25 (55.56) | 20 (44.44) | | 29 (64.44) | 16 (35.56) | |
| N1 | 14 (43.75) | 18 (56.25) | | 10 (31.25) | 22 (68.75) | |
| TNM stage[c] | | | 0.915 | | | 0.029[b] |
| I | 18 (50.00) | 18 (50.00) | | 23 (63.89) | 13 (36.11) | |
| II-IV | 21 (51.22) | 20 (48.78) | | 16 (39.02) | 25 (60.98) | |

[a]1 case lacked information; [b]P<0.05; [c]5 cases lacked information; [d]P<0.01. CD, cluster of differentiation; CTLs, cytotoxic T lymphocytes; Tregs, T regulatory cells.

TME (33). Accumulating evidence has shown that Tregs are involved in multiple immunoregulatory mechanisms and execute functions of the host immune response (33,34). Tregs mediate tumor cells to evade immune surveillance and immune elimination, and to promote the progression of malignant tumors (26,33,34). The $FOXP3^+$ Treg infiltrate in the TME can inhibit the function of effector T cells and dendritic cells by secreting suppressive cytokines, such as IL-10 and TGF-β, or via the cell-mediated involvement of inhibitory receptors, promoting the exhaustion of effector T cells (35). Previous studies revealed that the number of Tregs was significantly increased in a variety of tumor tissues, including ovarian, colorectal and lung cancer (31,36,37). In the case of PC, the density of Tregs was significantly higher in tumor tissues than that noted in the paratumoral pancreatic tissues. The density of Tregs was significantly correlated with the histological grade and lymph node metastasis (38). In a consecutive series of 92 patients with PC resection, Liu *et al* (39) demonstrated that patients with higher levels of intratumoral Tregs exhibited shorter DFS times than those with lower levels of Tregs (11.2 vs. 22.2 months; P<0.001). In the current study, the data confirmed that the number of Tregs in PC tissues was significantly higher than that noted in paracancerous tissues; patients with lymph node metastasis and advanced TNM stage exhibited a higher level of Treg infiltrate in tumor tissues. Furthermore, higher Treg infiltrate was associated with a poorer prognosis in patients with PC, suggesting that this marker is an independent risk factor for the prognosis of this disease.

It is well established that immune checkpoints are important mechanisms for tumor immune escape (40,41). The PD-1/PD-L1 pathway is a major immune checkpoint for the tumor-suppressing function of the lymphocytes present within the TME (42). The PD-1/PD-L1 axis is an important target for tumor immunotherapy and PD-1/PD-L1 blockade has shown favorable therapeutic effects in a variety of cancer types (21,42,43). PD-1 is primarily expressed in activated $CD4^+$ T cells, $CD8^+$ T and B cells (44). However, PD-L1 is not only expressed in various immune cells, including activated $CD4^+$ T cells and Treg subsets, but also in tissue cells, including cancer cells (45,46). Previous studies have demonstrated that tumor cells and the TME can upregulate PD-L1 expression, activate PD-1/PD-L1 signaling pathways, and inhibit the activation and proliferation of $CD4^+$ and $CD8^+$ T cells. In addition, PD-1 binds to PD-L1 and acts on several key molecules in the T cell receptor-signaling pathway to inhibit the transcription and translation of genes

Table VII. Association between the percentage of PD-1$^+$ T cells and PD-L1$^+$ T cells with the clinicopathological characteristics in the 82 cases of pancreatic cancer.

| | PD-1$^+$ T cells, n (%) | | | PD-L1$^+$ T cells, n (%) | | |
|---|---|---|---|---|---|---|
| Variables | Low (n=41) | High (n=41) | P-value | Low (n=41) | High (n=41) | P-value |
| Sex | | | 0.488 | | | 0.488 |
| Male | 25 (47.17) | 28 (52.83) | | 28 (52.83) | 25 (47.17) | |
| Female | 16 (55.17) | 13 (44.83) | | 13 (44.83) | 16 (55.17) | |
| Age, years | | | 0.824 | | | 0.824 |
| ≤60 | 18 (48.65) | 19 (51.35) | | 19 (51.35) | 18 (48.65) | |
| >60 | 23 (51.11) | 22 (48.89) | | 22 (48.89) | 23 (51.11) | |
| Diameter, cm[a] | | | 0.245 | | | 0.752 |
| ≤3 | 9 (39.13) | 14 (60.87) | | 11 (47.83) | 12 (52.17) | |
| >3 | 31 (53.45) | 27 (46.55) | | 30 (51.72) | 28 (48.28) | |
| Differentiation | | | 0.012[b] | | | 0.494 |
| Well, moderately and highly differentiated | 20 (39.22) | 31 (60.78) | | 24 (47.06) | 27 (52.94) | |
| Poorly differentiated | 21 (67.74) | 10 (32.26) | | 17 (54.84) | 14 (45.16) | |
| T stage[a] | | | 0.027 | | | 0.615 |
| T1/T2 | 28 (43.08) | 37 (56.92) | | 32 (49.23) | 33 (50.77) | |
| T3 | 12 (75.00) | 4 (25.00) | | 9 (56.25) | 7 (43.75) | |
| N stage[c] | | | 0.079 | | | 0.002[d] |
| N0 | 26 (57.78) | 19 (42.22) | | 30 (66.67) | 15 (33.33) | |
| N1 | 12 (37.50) | 20 (62.50) | | 10 (31.25) | 22 (68.75) | |
| TNM stage[c] | | | 0.726 | | | 0.015[b] |
| I | 17 (47.22) | 19 (52.78) | | 24 (66.67) | 12 (33.33) | |
| II-IV | 21 (51.22) | 20 (48.78) | | 16 (39.02) | 25 (60.98) | |

[a]1 case lacked information; [b]P<0.05; [c]5 cases lacked information; [d]P<0.01. PD-1, programmed cell death protein 1; PD-L1, programmed cell death ligand 1.

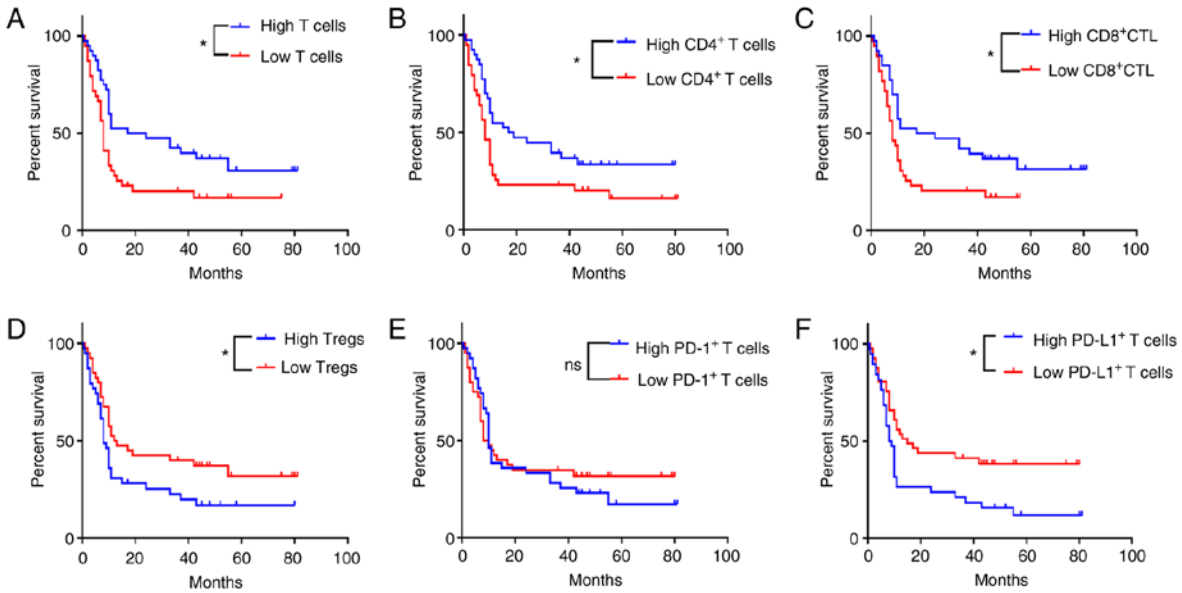


Figure 3. Associations of TIL types with disease prognosis. Kaplan-Meier analysis (A-F) indicated that patients with high infiltrates of (A) total T cells, (B) CD4$^+$ T cells and (C) CD8$^+$ CTLs exhibited a significantly longer OS time than those with low levels of infiltrates. By contrast, the OS times of patients with low levels of (D) Tregs and (F) PD-L1$^+$ T cell infiltrates was significantly shorter; the infiltrate levels of (E) PD-1$^+$ T cells exhibited no significant effect on the OS. *P<0.05. ns, no significance; TIL, tumor-infiltrating lymphocyte; CD, cluster of differentiation; CTLs, cytotoxic T lymphocytes; OS, overall survival; Treg, T regulatory cell; PD-L1, programmed cell death ligand 1; PD-1, programmed cell death protein 1.

Table VIII. Single factor analysis of prognosis in the 82 cases of pancreatic cancer.

| Clinicopathological parameters | n | Hazard ratio | 95% confidence interval | P-value |
|---|---|---|---|---|
| Sex | | 1.037 | 0.557-4.248 | 0.409 |
| Male | 53 | | | |
| Female | 29 | | | |
| Age, years | | 1.149 | 0.474-3.516 | 0.369 |
| ≤60 | 37 | | | |
| >60 | 45 | | | |
| Diameter, cm[a] | | 1.391 | 0.301-8.419 | 0.540 |
| ≤3 | 23 | | | |
| >3 | 58 | | | |
| Differentiation | | 2.354 | 1.046-15.924 | 0.010[b] |
| Well/moderately differentiated | 51 | | | |
| Poorly differentiated | 31 | | | |
| T-stage[a] | | 0.233 | 0.043-1.260 | 0.996 |
| T1/T2 | 65 | | | |
| T3 | 16 | | | |
| N-stage[c] | | 5.869 | 1.548-22.251 | 0.007[b] |
| N0 | 45 | | | |
| N1 | 32 | | | |
| TNM stage[c] | | 3.712 | 1.242-11.096 | 0.004[b] |
| I | 36 | | | |
| II-IV | 41 | | | |
| Total T cells | | 2.634 | 1.347-18.354 | 0.010[b] |
| High | 41 | | | |
| Low | 41 | | | |
| $CD4^+$ T cells | | 1.926 | 1.152-16.327 | 0.021[d] |
| High | 41 | | | |
| Low | 41 | | | |
| $CD8^+$ CTLs | | 2.015 | 1.065-19.083 | 0.015[d] |
| High | 41 | | | |
| Low | 41 | | | |
| Tregs | | 1.375 | 1.013-8.419 | 0.036[d] |
| High | 41 | | | |
| Low | 41 | | | |
| PD-$1^+$ T cells | | 0.915 | 0.694-5.282 | 0.677 |
| High | 41 | | | |
| Low | 41 | | | |
| PD-$L1^+$ T cells | | 4.608 | 1.494-34.213 | 0.005[b] |
| High | 41 | | | |
| Low | 41 | | | |

[a]1 case lacked information; [b]P≤0.01; [c]5 cases lacked information; [d]P≤0.05. PD-1, programmed cell death protein 1; PD-L1, programmed cell death ligand 1; CD, cluster of differentiation; CTLs, cytotoxic T lymphocytes; Tregs, T regulatory cells.

and cytokines required for T-cell activation. Moreover, it induces T-cell apoptosis, thereby negatively regulating the body's immune response (47,48). Moreover, activation of the PD-1/PD-L1 signaling pathway can also maintain the function of the Tregs and promote their development (49,50). Wang *et al* (51) indicated that high expression of PD-1 on the membranes of T cells was significantly correlated with optimal differentiation and advanced T stage in PC, whereas high expression of PD-1 indicated a significantly superior OS rate. Nevertheless, in the current study, it was found that the number of PD-$1^+$ T cells exhibited no significant difference between PC and paracancerous tissues. Although the infiltrate

Table IX. Multivariate analysis of prognosis in 82 cases of pancreatic cancer.

| Clinicopathological parameters | n | Hazard ratio | 95% confidence interval | P-value |
|---|---|---|---|---|
| Differentiation | | 2.733 | 1.491-5.009 | 0.001[a] |
| Well | 51 | | | |
| Moderately | 31 | | | |
| N stage[b] | | 2.243 | 0.794-6.332 | 0.127 |
| N0 | 45 | | | |
| N1 | 32 | | | |
| TNM stage[b] | | 2.364 | 1.297-4.308 | 0.005[c] |
| I | 36 | | | |
| II-IV | 41 | | | |
| Total T cells | | 0.323 | 0.169-0.618 | 0.001[a] |
| High | 41 | | | |
| Low | 41 | | | |
| $CD4^+$ T cells | | 0.393 | 0.214-0.722 | 0.003[c] |
| High | 41 | | | |
| Low | 41 | | | |
| $CD8^+$ CTLs | | 0.587 | 0.303-1.137 | 0.114 |
| High | 41 | | | |
| Low | 41 | | | |
| Tregs | | 2.786 | 1.426-5.445 | 0.003[c] |
| High | 41 | | | |
| Low | 41 | | | |
| PD-$L1^+$ T cells | | 2.305 | 1.205-4.409 | 0.012[d] |
| High | 41 | | | |
| Low | 41 | | | |

[a]P≤0.001; [b]5 cases lacked information; [c]P≤0.01; [d]P≤0.05. CD, cluster of differentiation; CTLs, cytotoxic T lymphocytes; Tregs, T regulatory cells.

level of PD-$1^+$ T cells was lower in patients with poor differentiation and advanced T stage, it did not cause a significant effect on the OS rate of patients with PC. PD-1 is expressed on the surface of activated T cells in PC tissues, mostly $CD4^+$ T cells and $CD8^+$ T cells, as well as B cells and monocytes. At the same time, activated T cells are inhibited in the tumor immune microenvironment, and PD-L1 expressed in PC cells can transmit negative regulatory signals after binding with PD-1, which leads to a reduction in T-cell proliferation or apoptosis while cancer cells exhibit rapid growth (5). This may well explain why there was no significant difference in PD-1 expression between PC and adjacent normal tissues in the present study. Previous studies indicated that PD-L1 was abnormally upregulated in tumor tissues of lung cancer and melanoma, while PD-L1 expression was significantly associated with improved outcomes and therapeutic responses to anti-PD-L1 antibody treatments (52,53). Based on the mRNA expression data from TCGA and the immunohistochemical protein expression data derived from 33 cases of PC, Danilova *et al* (54) indicated that PD-L1 expression in PC was associated with CD8A expression, IDO1 expression and the Th1/IFN-γ gene signature. Moreover, high PD-L1 expression was associated with poor patient survival in patients with PC. The results of the present study suggested that the number of PD-$L1^+$ T cells was markedly higher in PC tissues than that noted in paracancerous tissues. A higher infiltrate of PD-$L1^+$ T cells was noted in patients with positive lymph nodes and advanced TNM stage, which supported a lower survival time for patients with PC and a higher PD-$L1^+$ T cell infiltrate.

Undoubtedly, the present study has certain limitations. Firstly, not all types of TILs were investigated, the spatial distribution characteristics of TILs were not described and the results of RT-qPCR for TIL expression are lacking. Secondly, the detection of TILs was based on a commercial TMA with limited cases, and certain clinicopathological data were omitted, such as pancreatolithiasis, drinking habits, and history of chronic pancreatitis and type 2 diabetes. Thirdly, other immunosuppressive cells that regulate the infiltration of TILs in the pancreatic TME, such as M2-like TAMs, MDSCs and cancer-associated fibroblasts, were not involved in the present study. Therefore, additional large-scale studies are required to further improve these limitations.

In summary, the results of the present study demonstrated that patients with PC had an immunosuppressive TME, with reduced numbers of $CD4^+$ T cells and reduced levels of $CD8^+$ CTL infiltrates, as well as increased numbers of Tregs and PD-$L1^+$ T cells. The infiltrates of total T cells, $CD4^+$ T cells, Tregs and PD-$L1^+$ T cells in the TME were independent risk

factors for the prognosis of PC. These TILs are expected to be novel targets for remodeling the TME of PC.

**Acknowledgements**

Not applicable.

**Funding**

The present study was supported by the National Natural Science Foundation of China (grant no. 81860418), the Natural Science Foundation of Jiangxi Province (grant no. 20202ACB206007), and the Key Research and Development Program of Jiangxi Province (grant no. 20192BBG70035).

**Availability of data and materials**

The datasets used and/or analyzed during the current study are available from the corresponding author on reasonable request.

**Authors' contributions**

WX conceived and designed the study. GS, ZY, KF and ST performed the experiments and wrote the manuscript. YX and SY acquired and analyzed the data. GS and WX edited and revised the manuscript. All authors have read and approved the final manuscript.

**Ethics approval and consent to participate**

The present study was approved by the Ethics Committee of the First Affiliated Hospital of Nanchang University [approval no. (2021) 42; Nanchang, China].

**Patient consent for publication**

The creation and use of TMA were approved by the Ethics Committee of Shanghai Outdo Biotech Co., Ltd. (approval no. YB M-05-02).

**Competing interests**

The authors declare that they have no competing interests.

**References**

1. Xia C, Dong X, Li H, Cao M, Sun D, He S, Yang F, Yan X, Zhang S, Li N and Chen W: Cancer statistics in China and United States, 2022: Profiles, trends, and determinants. Chin Med J (Engl) 135: 584-590, 2022.
2. Siegel RL, Miller KD, Fuchs HE and Jemal A: Cancer statistics, 2022. CA Cancer J Clin 72: 7-33, 2022.
3. Rahib L, Smith BD, Aizenberg R, Rosenzweig AB, Fleshman JM and Matrisian LM: Projecting cancer incidence and deaths to 2030: The unexpected burden of thyroid, liver, and pancreas cancers in the United States. Cancer Res 74: 2913-2921, 2014.
4. Spill F, Reynolds DS, Kamm RD and Zaman MH: Impact of the physical microenvironment on tumor progression and metastasis. Curr Opin Biotechnol 40: 41-48, 2016.
5. Wang S, Li Y, Xing C, Ding C, Zhang H, Chen L, You L, Dai M and Zhao Y: Tumor microenvironment in chemoresistance, metastasis and immunotherapy of pancreatic cancer. Am J Cancer Res 10: 1937-1953, 2020.
6. Hinshaw DC and Shevde LA: The tumor microenvironment innately modulates cancer progression. Cancer Res 79: 4557-4566, 2019.
7. Fu X, Sun G, Tu S, Fang K, Xiong Y, Tu Y, Zha M, Xiao T and Xiao W: Hsa_circ_0046523 mediates an immunosuppressive tumor microenvironment by regulating MiR-148a-3p/PD-L1 axis in pancreatic cancer. Front Oncol 12: 877376, 2022.
8. Kaneda MM, Messer KS, Ralainirina N, Li H, Leem CJ, Gorjestani S, Woo G, Nguyen AV, Figueiredo CC, Foubert P, *et al*: PI3Kγ is a molecular switch that controls immune suppression. Nature 539: 437-442, 2016.
9. Kabashima A, Matsuo Y, Ito S, Akiyama Y, Ishii T, Shimada S, Masamune A, Tanabe M and Tanaka S: cGAS-STING signaling encourages immune cell overcoming of fibroblast barricades in pancreatic cancer. Sci Rep 12: 10466, 2022.
10. Lefler JE, MarElia-Bennett CB, Thies KA, Hildreth BE III, Sharma SM, Pitarresi JR, Han L, Everett C, Koivisto C, Cuitino MC, *et al*: STAT3 in tumor fibroblasts promotes an immunosuppressive microenvironment in pancreatic cancer. Life Sci Alliance 5: e202201460, 2022.
11. Nejati R, Goldstein JB, Halperin DM, Wang H, Hejazi N, Rashid A, Katz MH, Lee JE, Fleming JB, Rodriguez-Canales J, *et al*: Prognostic significance of tumor-infiltrating lymphocytes in patients with pancreatic ductal adenocarcinoma treated with neoadjuvant chemotherapy. Pancreas 46: 1180-1187, 2017.
12. Hivroz C, Chemin K, Tourret M and Bohineust A: Crosstalk between T lymphocytes and dendritic cells. Crit Rev Immunol 32: 139-155, 2012.
13. Wang T, Niu G, Kortylewski M, Burdelya L, Shain K, Zhang S, Bhattacharya R, Gabrilovich D, Heller R, Coppola D, *et al*: Regulation of the innate and adaptive immune responses by Stat-3 signaling in tumor cells. Nat Med 10: 48-54, 2004.
14. Orhan A, Vogelsang RP, Andersen MB, Madsen MT, Hölmich ER, Raskov H and Gögenur I: The prognostic value of tumour-infiltrating lymphocytes in pancreatic cancer: a systematic review and meta-analysis. Eur J Cancer 132: 71-84, 2020.
15. Biswas SK and Mantovani A: Macrophage plasticity and interaction with lymphocyte subsets: Cancer as a paradigm. Nat Immunol 11: 889-896, 2010.
16. Hu L, Zhu M, Shen Y, Zhong Z and Wu B: The prognostic value of intratumoral and peritumoral tumor-infiltrating FoxP3+Treg cells in of pancreatic adenocarcinoma: A meta-analysis. World J Surg Oncol 19: 300, 2021.
17. Thompson RH, Dong H, Lohse CM, Leibovich BC, Blute ML, Cheville JC and Kwon ED: PD-1 is expressed by tumor-infiltrating immune cells and is associated with poor outcome for patients with renal cell carcinoma. Clin Cancer Res 13: 1757-1761, 2007.
18. Ahmadzadeh M, Johnson LA, Heemskerk B, Wunderlich JR, Dudley ME, White DE and Rosenberg SA: Tumor antigen-specific CD8 T cells infiltrating the tumor express high levels of PD-1 and are functionally impaired. Blood 114: 1537-1544, 2009.
19. Nomi T, Sho M, Akahori T, Hamada K, Kubo A, Kanehiro H, Nakamura S, Enomoto K, Yagita H, Azuma M and Nakajima Y: Clinical significance and therapeutic potential of the programmed death-1 ligand/programmed death-1 pathway in human pancreatic cancer. Clin Cancer Res 13: 2151-2157, 2007.
20. Court CM and Hines OJ: The new American joint committee on cancer TNM staging system for pancreatic cancer-balancing usefulness with prognostication. JAMA Surg 153: e183629, 2018.
21. Wang X, Teng F, Kong L and Yu J: PD-L1 expression in human cancers and its association with clinical outcomes. Onco Targets Ther 12: 5023-5039, 2016.
22. Shi F, Shi M, Zeng Z, Qi RZ, Liu ZW, Zhang JY, Yang YP, Tien P and Wang FS: PD-1 and PD-L1 upregulation promotes CD8(+) T-cell apoptosis and postoperative recurrence in hepatocellular carcinoma patients. Int J Cancer 128: 887-896, 2011.
23. Ino Y, Yamazaki-Itoh R, Shimada K, Iwasaki M, Kosuge T, Kanai Y and Hiraoka N: Immune cell infiltration as an indicator of the immune microenvironment of pancreatic cancer. Br J Cancer 108: 914-923, 2013.
24. Reading JL, Gálvez-Cancino F, Swanton C, Lladser A, Peggs KS and Quezada SA: The function and dysfunction of memory $CD8^+$ T cells in tumor immunity. Immunol Rev 283: 194-212, 2018.
25. Shrihari TG: Innate and adaptive immune cells in Tumor microenvironment. Gulf J Oncolog 1: 77-81, 2021.
26. Tang Y, Xu X, Guo S, Zhang C, Tang Y, Tian Y, Ni B, Lu B and Wang H: An increased abundance of tumor-infiltrating regulatory T cells is correlated with the progression and prognosis of pancreatic ductal adenocarcinoma. PLoS One 9: e91551, 2014.

27. Masugi Y, Abe T, Ueno A, Fujii-Nishimura Y, Ojima H, Endo Y, Fujita Y, Kitago M, Shinoda M, Kitagawa Y and Sakamoto M: Characterization of spatial distribution of tumor-infiltrating $CD8^+$ T cells refines their prognostic utility for pancreatic cancer survival. Mod Pathol 32: 1495-1507, 2019.
28. Karakhanova S, Ryschich E, Mosl B, Harig S, Jäger D, Schmidt J, Hartwig W, Werner J and Bazhin AV: Prognostic and predictive value of immunological parameters for chemoradioimmunotherapy in patients with pancreatic adenocarcinoma. Br J Cancer 112: 1027-1036, 2015.
29. de Vos van Steenwijk PJ, Ramwadhdoebe TH, Goedemans R, Doorduijn EM, van Ham JJ, Gorter A, van Hall T, Kuijjer ML, van Poelgeest MI, van der Burg SH and Jordanova ES: Tumor-infiltrating CD14-positive myeloid cells and CD8-positive T-cells prolong survival in patients with cervical carcinoma. Int J Cancer 133: 2884-2894, 2013.
30. Preston CC, Maurer MJ, Oberg AL, Visscher DW, Kalli KR, Hartmann LC, Goode EL and Knutson KL: The ratios of $CD8^+$ T cells to $CD4^+CD25^+$ $FOXP3^+$ and FOXP3-T cells correlate with poor clinical outcome in human serous ovarian cancer. PLoS One 8: e80063, 2013.
31. Timperi E, Pacella I, Schinzari V, Focaccetti C, Sacco L, Farelli F, Caronna R, Del Bene G, Longo F, Ciardi A, *et al*: Regulatory T cells with multiple suppressive and potentially pro-tumor activities accumulate in human colorectal cancer. Oncoimmunology 5: e1175800, 2016.
32. Revilla SA, Kranenburg O and Coffer PJ: Colorectal cancer-infiltrating regulatory T cells: Functional heterogeneity, metabolic adaptation, and therapeutic targeting. Front Immunol 13: 903564, 2022.
33. Itahashi K, Irie T and Nishikawa H: Regulatory T-cell development in the tumor microenvironment. Eur J Immunol 52: 1216-1227, 2022.
34. Zhang Y, Lazarus J, Steele NG, Yan W, Lee HJ, Nwosu ZC, Halbrook CJ, Menjivar RE, Kemp SB and Sirihorachai VR: Regulatory T-cell depletion alters the tumor microenvironment and accelerates pancreatic carcinogenesis. Cancer Discov 10: 422-439, 2020.
35. Saka D, Gökalp M, Piyade B, Cevik NC, Sever EA, Unutmaz D, Ceyhan GO, Demir IE and Asimgil H: Mechanisms of T-cell exhaustion in pancreatic cancer. Cancers (Basel) 12: 2274, 2020.
36. Kampan NC, Madondo MT, McNally OM, Stephens AN, Quinn MA and Plebanski M: Interleukin 6 present in inflammatory ascites from advanced epithelial ovarian cancer patients promotes tumor necrosis factor receptor 2-expressing regulatory T cells. Front Immunol 8: 1482, 2017.
37. Woo EY, Chu CS, Goletz TJ, Schlienger K, Yeh H, Coukos G, Rubin SC, Kaiser LR and June CH: Regulatory CD4(+)CD25(+) T cells in tumors from patients with early-stage non-small cell lung cancer and late-stage ovarian cancer. Cancer Res 61: 4766-4772, 2001.
38. Jiang Y, Du Z, Yang F, Di Y, Li J, Zhou Z, Pillarisetty VG and Fu D: FOXP3+ lymphocyte density in pancreatic cancer correlates with lymph node metastasis. PLoS One 9: e106741, 2014.
39. Liu L, Zhao G, Wu W, Rong Y, Jin D, Wang D, Lou W and Qin X: Low intratumoral regulatory T cells and high peritumoral CD8(+) T cells relate to long-term survival in patients with pancreatic ductal adenocarcinoma after pancreatectomy. Cancer Immunol Immunother 65: 73-82, 2016.
40. Steele NG, Carpenter ES, Kemp SB, Sirihorachai VR, The S, Delrosario L, Lazarus J, Amir ED, Gunchick V, Espinoza C, *et al*: Multimodal mapping of the tumor and peripheral blood immune landscape in human pancreatic cancer. Nat Cancer 1: 1097-1112, 2020.
41. Schizas D, Charalampakis N, Kole C, Economopoulou P, Koustas E, Gkotsis E, Ziogas D, Psyrri A and Karamouzis MV: Immunotherapy for pancreatic cancer: A 2020 update. Cancer Treat Rev 86: 102016, 2020.
42. Feng M, Xiong G, Cao Z, Yang G, Zheng S, Song X, You L, Zheng L, Zhang T and Zhao Y: PD-1/PD-L1 and immunotherapy for pancreatic cancer. Cancer Lett 407: 57-65, 2017.
43. Liang X, Sun J, Wu H, Luo Y, Wang L, Lu J, Zhang Z, Guo J, Liang Z and Liu T: PD-L1 in pancreatic ductal adenocarcinoma: A retrospective analysis of 373 Chinese patients using an in vitro diagnostic assay. Diagn Pathol 13: 5, 2018.
44. Ishida Y, Agata Y, Shibahara K and Honjo T: Induced expression of PD-1, a novel member of the immunoglobulin gene superfamily, upon programmed cell death. EMBO J 11: 3887-3895, 1992.
45. Ishida M, Iwai Y, Tanaka Y, Okazaki T, Freeman GJ, Minato N and Honjo T: Differential expression of PD-L1 and PD-L2, ligands for an inhibitory receptor PD-1, in the cells of lymphohematopoietic tissues. Immunol Lett 84: 57-62, 2002.
46. Eppihimer MJ, Gunn J, Freeman GJ, Greenfield EA, Chernova T, Erickson J and Leonard JP: Expression and regulation of the PD-L1 immunoinhibitory molecule on microvascular endothelial cells. Microcirculation 9: 133-145, 2002.
47. Zhou WY, Zhang MM, Liu C, Kang Y, Wang JO and Yang XH: Long noncoding RNA LINC00473 drives the progression of pancreatic cancer via upregulating programmed death-ligand 1 by sponging microRNA-195-5p. J Cell Physiol 234: 23176-23189, 2019.
48. Lee A, Lim S, Oh J, Lim J, Yang Y, Lee MS and Lim JS: NDRG2 expression in breast cancer cells downregulates PD-L1 expression and restores T cell proliferation in tumor-coculture. Cancers (Basel) 13: 6112, 2021.
49. Que Y, Xiao W, Guan YX, Liang Y, Yan SM, Chen HY, Li QQ, Xu BS, Zhou ZW and Zhang X: PD-L1 expression is associated with FOXP3+ regulatory T-cell infiltration of soft tissue sarcoma and poor patient prognosis. J Cancer 8: 2018-2025, 2017.
50. Chen JX, Yi XJ, Gao SX and Sun JX: The possible regulatory effect of the PD-1/PD-L1 signaling pathway on Tregs in ovarian cancer. Gen Physiol Biophys 39: 319-330, 2020.
51. Wang Y, Lin J, Cui J, Han T, Jiao F, Meng Z and Wang L: Prognostic value and clinicopathological features of PD-1/PD-L1 expression with mismatch repair status and desmoplastic stroma in Chinese patients with pancreatic cancer. Oncotarget 8: 9354-9365, 2017.
52. Velcheti V, Schalper KA, Carvajal DE, Anagnostou VK, Syrigos KN, Sznol M, Herbst RS, Gettinger SN, Chen L and Rimm DL: Programmed death ligand-1 expression in non-small cell lung cancer. Lab Invest 94: 107-116, 2014.
53. Soliman H, Khalil F and Antonia S: PD-L1 expression is increased in a subset of basal type breast cancer cells. PLoS One 9: e88557, 2014.
54. Danilova L, Ho WJ, Zhu Q, Vithayathil T, De Jesus-Acosta A, Azad NS, Laheru DA, Fertig EJ, Anders R, Jaffee EM and Yarchoan M: Programmed cell death ligand-1 (PD-L1) and CD8 expression profiling identify an immunologic subtype of pancreatic ductal adenocarcinomas with favorable survival. Cancer Immunol Res 7: 886-895, 2019.